

**MICROPOROUS AND MESOPOROUS
MATERIALS: FORMATION STUDY,
PROPERTIES INVESTIGATION AND
CATALYTIC BEHAVIOR IN ALDOL
CONDENSATION OF HEPTANAL AND
BENZALDEHYDE**

ABDULLAHI HARUNA

**UNIVERSITI SAINS MALAYSIA
2019**

**MICROPOROUS AND MESOPOROUS
MATERIALS: FORMATION STUDY,
PROPERTIES INVESTIGATION AND
CATALYTIC BEHAVIOR IN ALDOL
CONDENSATION OF HEPTANAL AND
BENZALDEHYDE**

by

ABDULLAHI HARUNA

**Thesis submitted in fulfillment of the requirement
for the degree of
Doctor of Philosophy**

November 2019

ACKNOWLEDGEMENT

I would like to use this opportunity to express my genuine appreciation to my supervisor, Assoc. Prof. Dr. Ng Eng Poh, for his skilled guidance, assistance, immense contribution and valuable suggestions, encouragement towards the realization of this study. His vast knowledge helps me a lot throughout my research work. I would also like to acknowledge Universiti Sains Malaysia, Nanyang Technological University (Singapore), Université de Haute-Alsace (France) and Universiti of Malaya for the availability of the needed facilities which enable the success of my project. I would extend my appreciation to FRGS (203/PKIMIA/6711495) and RUI (1001/PKIMIA/8011012) research grants, Tertiary Education Trust Fund (TETFund), Federal University Dutsin-ma for their financial support that allows me to do this research. Special thanks go to all academic and non-academic staff of School of Chemical Sciences, USM that have contributed enormously throughout the period of my research. My earnest gratitude goes to my lab mates Ms. Nurhidayahni, Mrs. Tamara, Mrs. Ghadah, Ms. Cythia and Mr. Ismail H. for their huge support, guidance and encouragement toward attaining the desired goal. Last but not least, my sincere appreciation dedicates to my parent, my brothers and my family for their love, support, patience and faith in me. This also contributes largely to the accomplishment of my PhD journey.

TABLE OF CONTENTS

ACKNOWLEDGEMENT	ii
TABLE OF CONTENTS	iii
LIST OF TABLES	viii
LIST OF FIGURES	ix
LIST SYMBOLS AND NOMENCLATURES	xiv
LIST OF ABBREVIATIONS	xv
ABSTRAK	xvi
ABSTRACT	xviii

CHAPTER ONE - INTRODUCTION

1.1 General introduction	1
1.2 Development of zeotype solid base catalysts	2
1.3 Aims of the study	4
1.4 Objectives of the study	5
1.5 Scope of the thesis	7

CHAPTER TWO - LITERATURE STUDY

2.1 Microporous zeolite and zeotype solids	9
2.2 Nankai Number 2 aluminophosphate (NKX-2)	11
2.2.1 Synthesis of NKX-2	13
2.3 MCM-41 mesoporous molecular sieves	13
2.3.1 Synthesis and formation of MCM-41	16
2.3.2 Generation of catalytic active sites on MCM-41	17
2.4 Synthesis of jasminaldehyde via catalytic aldol condensation of benzaldehyde with heptanal	20
2.5 Heating methods	24

2.5.1	Reflux heating.....	24
2.5.2	Microwave heating	25
2.5.3	Non-microwave instant heating.....	26
2.6	Characterization techniques.....	27
2.6.1	X-ray diffraction (XRD) analysis	28
2.6.2.	Transmission electron microscopy (TEM).....	29
2.6.3	Fourier transform infrared (FTIR) spectroscopy	31
2.6.4	Solid-state magic angle spinning nuclear magnetic resonance spectroscopy (MAS NMR).....	33
2.6.5	Nitrogen (N ₂) gas adsorption-desorption analysis.....	35
2.6.6	Field emission scanning electron microscopy (FESEM).....	38
2.6.7	Energy-dispersive X-ray (EDX) spectroscopy	39
2.6.8	Inductively coupled plasma optical emission spectrometry (ICP-OES).....	40
2.6.9	Pyrrole adsorption.....	40
2.6.10	Temperature-programmed desorption of carbon dioxide (TPD-CO ₂)..	41
2.6.11	Thermogravimetry/Differential Thermogravimetry (TGA/DTG)	41
2.6.12	X-ray fluorescence (XRF) spectroscopy.....	42
2.6.13	Gas chromatography (GC) analysis.....	43
2.6.14	Gas chromatography-mass spectrometry (GC-MS)	44

CHAPTER THREE - MATERIALS AND EXPERIMENTAL METHODS

3.1	Introduction.....	46
3.2	Chemicals	46
3.3	Formation study of ultrasmall CsMCM-41 hollow nanospheres	47
3.4	Synthesis of CsMCM-41 with different Al contents	47
3.5	Synthesis of Li-, Na-, K- and Cs-AlMCM-41 mesoporous materials	48
3.6	Hydrothermal synthesis of M-NKX-2 crystals (M = Li, Na, K, Cs).....	49

3.7	Characterization.....	49
3.8	Catalytic aldol condensation of heptanal and benzaldehyde	51

CHAPTER FOUR - A TIME DEPENDANT STUDY OF THE FORMATION OF ULTRASMALL CS-ALMCM-41 HOLLOW NANOSPHERES

4.1	Introduction.....	53
4.2	Results and discussion	54
4.3	Summary.....	65

CHAPTER FIVE - ULTRASMALL CS-ALMCM-41 BASIC CATALYSTS: EFFECTS OF ALUMINUM ADDITION ON THEIR PHYSICO-CHEMICAL AND CATALYTIC PROPERTIES

5.1	Introduction.....	66
5.2	Results and discussion	67
5.2.1	Effects of Al content on the formation of ultrasmall CsMCM-41 nanoparticles monitored by FTIR spectroscopy and thermogravimetry analysis.....	67
5.2.2	Structural, morphological and porous characterizations.....	71
5.2.3	Elemental and surface basicity characterizations	77
5.2.4	Catalytic study	84
5.2.4(a)	Effect of SiO ₂ /Al ₂ O ₃ molar ratio	84
5.2.4(b)	Effects of reaction temperature and microwave heating time	85
5.2.4(c)	Effect of catalyst loading.....	86
5.2.4(d)	Influence of heptanal:benzaldehyde feed molar ratio	88
5.2.4(e)	Effect of solvent	89
5.2.4(f)	Catalytic comparative study	90
5.2.4(g)	Catalyst reusability test	90

CHAPTER SIX - MINERALIZER EFFECTS ON THE PHYSICOCHEMICAL AND CATALYTIC PROPERTIES OF ALMCM-41 MESOPOROUS MATERIALS

6.1	Introduction.....	93
6.2	Results and discussion	94
6.2.1	Characterization of surface and structural properties	94
6.2.2	Elemental analysis and surface basicity.....	103
6.2.3	Catalytic reaction study	107
6.3	Reaction mechanism.....	109
6.4	Summary.....	113

CHAPTER SEVEN - EFFECTS OF VARIOUS ALKALI METAL CATIONS ON THE SYNTHESIS, CRYSTALLIZATION AND CATALYTIC PROPERTIES OF NKX-2 ALUMINOPHOSPHITES

7.1	Introduction.....	114
7.2	Results and discussion	115
7.2.1	Synthesis of M-NKX-2 (M = Li, Na, K, Cs)	115
7.2.2	Catalytic behaviour of MeNKX-2	126
7.2.2(a)	Effect of temperature on CsNKX-2	128
7.2.2(b)	Effect of heptanal to benzaldehyde molar ratio	129
7.2.2(c)	Catalyst comparative study	130
7.2.2(d)	Catalyst reusability.....	132
7.3	Summary.....	133

CHAPTER EIGHT - CONCLUSIONS AND FUTURE WORKS

8.1	Conclusions	134
8.2	Recommendations of future works.....	136

REFERENCES..... 138

APPENDICES

LIST OF PUBLICATIONS

LIST OF TABLES

	Page
Table 2.1	Members of M41s mesoporous materials (Murugavel et al, 2008; Alothman, 2012)..... 15
Table 2.2	Aldol condensation catalyzed using of various solid acid and base catalyts under reflux condition. 24
Table 2.3	Possible vibration bands of zeolite framework in the IR region (400-1500 cm ⁻¹) (Kitsopoulos, 1999; Wan et al. 2016)..... 32
Table 4.1	Textural properties of the MCM-41 samples 55
Table 4.2	Chemical composition of samples heated at different times..... 64
Table 5.1	Thermogravimetry analysis data of as-synthesized CsMCM-41 nanoparticles..... 71
Table 5.2	Textural properties of the MCM-41 samples. 73
Table 5.3	Chemical elemental and basicity analyses of CsMCM-41 solids..... 78
Table 5.4	Effect of Al content in ultrasmall CsMCM-41 nanoparticles on the microwave-assisted aldol condensation reaction. ^a 85
Table 5.5	Effects of solvent on aldol condensation of benzaldehyde with heptanal..... 90
Table 5.6	Catalytic comparative study with closely related catalyst systems. 92
Table 6.1	Textural properties of the AlMCM-41 samples. 96
Table 6.2	Chemical compositions and basicity of Li-, Na-, K- and Cs-AlMCM-41 samples. 104
Table 6.3	Catalytic comparative study between Cs-AlMCM-41 hollow nanosphere and closely related catalyst systems. 111
Table 7.1	Crystal data of pure NKX-2 and M-NKX-2 from Rietveld refinement..... 118
Table 7.2	Properties of M-NKX-2 solid products. 124

LIST OF FIGURES

	Page
Figure 2.1	Arrangement of AlO_4 and SiO_4 tetrahedra, and metal cation ($\text{M}^+ = \text{Na}^+$ or K^+) in zeolite framework..... 9
Figure 2.2	Arrangement of PO_4 and AlO_4 in AlPO zeotype framework which have neutral framework..... 10
Figure 2.3	Crystal and chemical structure of NKX-2 (Gopal et al., 2016; Li et al., 2006). 12
Figure 2.4	Formation of MCM-41 via liquid crystal templating mechanism (Alothman, 2012). 17
Figure 2.5	Formation of Brönsted and Lewis acid sites in MCM-41 framework by isomorphous substitution of Al or other heteroatoms. 18
Figure 2.6	Preparation of highly basic Cs-AlMCM-41 via ion exchange of Na-AlMCM-41 using cesium acetate. 19
Figure 2.7	Generation of basic sites by functionalization of organosilane such as 3-aminopropyltriethoxysilane onto the surface of MCM-41 (Monnier et al., 1993). 19
Figure 2.8	Synthesis of jasminaldehyde using aldol condensation of benzaldehyde and heptanal. 20
Figure 2.9	Schematic diagram of reflux heating method (Karakassides et al. 2000). 25
Figure 2.10	Microwave heating caused by (a) ionic conduction and (b) dipolar interaction (Kappe, 2004). 26
Figure 2.11	Schematic diagram of non-microwave heating reactor (Ananth et al., 2012). 27
Figure 2.12	Geometry for the derivation of the Bragg equation where n is an integer, λ is the wavelength of the incident x-ray beams, d and θ are expressed as the interplanar distance between adjacent planes in a crystal and the diffraction angle between the scattering plane and the incident X-ray beams, respectively (Klug and Alexander, 1974). 29
Figure 2.13	A schematic diagram of transmission electron microscope (TEM). 31

Figure 2.14	²⁹ Si NMR chemical shift range. The Si(nAl) denotes the tetrahedra SiO ₄ connected to shared O atoms with tetrahedra n number of AlO ₄ in the aluminosilicate structure (Lippmaa et al., 1980; Lavalley, 1996).....	35
Figure 2.15	The adsorption isotherms according to IUPAC classification (AlOthman, 2012).	37
Figure 2.16	Types of hysteresis loops observed in the adsorption-desorption isotherms (AlOthman, 2012).....	37
Figure 2.17	A schematic diagram of FESEM microscope (Zhou and Wang, 2007).	39
Figure 2.18	A simple set-up of a gas chromatograph (GC) (Husain and Maqbool, 2014).	44
Figure 2.19	A gas chromatograph-mass spectrometer (GC-MS).	45
Figure 4.1	XRD patterns of solids after (a) 0 h, (b) 10 h, (c) 14 h and (d) 24 h of hydrothermal synthesis.	55
Figure 4.2	TEM images of Cs-ALMCM-41 solids after (a,b) 0 h, (c,d) 10 h, (e,f) 14 h and (g,h) 24 h of hydrothermal treatment.....	57
Figure 4.3	Yield of solids after (a) 0 h, (b) 10 h, (c) 14 h and (d) 24 h of hydrothermal heating.	58
Figure 4.4	FTIR spectra of as-synthesized Cs-ALMCM-41 solids after (a) 0 h, (b) 10 h, (c) 14 h and (d) 24 h of hydrothermal treatment.....	59
Figure 4.5	Thermograms of as-synthesized MCM-41 solids after (a) 0 h, (b) 10 h, (c) 14 h and (d) 24 h of hydrothermal treatment.	61
Figure 4.6	DTG curves of as-synthesized MCM-41 solids after (a) 0 h, (b)10 h, (c) 14 h and (d) 24 h of hydrothermal treatment.	61
Figure 4.7	N ₂ adsorption (close symbol) and desorption (open symbol) curves of (a) M-0h, (b) M-10h, (c) M-14h and (d) M-24h.	63
Figure 4.8	Pore size distribution of (a) M-0h, (b) M-10h, (c) M-14h and (d) M-24h.	63
Figure 5.1	IR spectra of as-synthesized (a) CsM-∞, (b) CsM-30, (c) CsM-20 and (d) CsM-5.	68
Figure 5.2	(A) TGA and (B) DTG profiles of as-synthesized (a) CsM-∞, (b) CsM-30, (c) CsM-20 and (d) CsM-5.	70

Figure 5.3	XRD patterns of calcined (a) CsM-∞, (b) CsM-30, (c) CsM-20 and (d) CsM-5.	72
Figure 5.4	5.1. TEM images of (a) CsM-∞, (b) CsM-30, (c) CsM-20 (d) CsM-5. The particle size distribution plots of (e) CsM-∞, (f) CsM-30, (g) CsM-20 and (h) CsM-5 are also shown.	75
Figure 5.5	N ₂ adsorption (close symbol) and desorption (open symbol) isotherms, and pore size distribution (inset) of calcined (a) CsM-∞, (b) CsM-30, (c) CsM-20 and (d) CsM-5 nanoparticles.	77
Figure 5.6	CO ₂ -TPD profiles of calcined (a) CsM-∞, (b) CsM-30, (c) CsM-20 and (d) CsM-5 nanoparticles.....	80
Figure 5.7	FTIR spectra of (a) CsM-∞, (b) CsM-30, (c) CsM-20 and (d) CsM-5 nanoparticles after being adsorbed with pyrrole.....	81
Figure 5.8	²⁷ Al solid state MAS NMR spectra of (a) uncalcined CsM-30, (b) calcined CsM-30, (c) uncalcined CsM-5 and (d) calcined CsM-5.	82
Figure 5.9	CP MAS ²⁹ Si MAS NMR spectra of uncalcined (a) CsM-∞, (b) CsM-30, (c) CsM-20 and (d) CsM-5.....	83
Figure 5.10	Effect of temperature and reaction time on heptanal conversion over the CsM-20 nanocatalyst at (a) 120 °C, (b) 140 °C, (c) 160 °C and (d) 180 °C. Inset: The selectivity to jasminaldehyde at 180 °C after 60 min of reaction.....	86
Figure 5.11	Conversion of heptanal and selectivity of jasminaldehyde catalyzed using different amounts of catalyst. Catalyst: CsM-20, heptanal:benzaldehyde feed molar ratio = 1:5, temperature = 180 °C, time = 60 min; microwave power = 800 W.	87
Figure 5.12	Conversion of heptanal and selectivity of jasminaldehyde using different heptanal:benzaldehyde molar ratios. Catalyst: CsM-20, catalyst loading = 0.500 g, temperature = 180 °C, time = 60 min; microwave power = 800 W.	89
Figure 6.1	XRD patterns of calcined (a) Li-ALMCM-41, (b) Na-ALMCM-41, (c) K-ALMCM-41 and (d) Cs-ALMCM-41.....	95
Figure 6.2	TEM images of calcined (a,b) Li-ALMCM-41, (c,d) Na-ALMCM-41, (e,f) K-ALMCM-41 and (g,h) Cs-ALMCM-41 with different magnifications.	99
Figure 6.3	N ₂ adsorption (close symbol) and desorption (open symbol) curves of (a) Li-ALMCM-41, (b) Na-ALMCM-41, (c) K-ALMCM-41 and (d) Cs-ALMCM-41.	100

Figure 6.4	Normalized pore size distribution of (a) Li- <i>AlMCM-41</i> , (b) Na- <i>AlMCM-41</i> , (c) K- <i>AlMCM-41</i> and (d) Cs- <i>AlMCM-41</i>	100
Figure 6.5	(A) TGA, (B) DTG profiles of calcined (a) Li- <i>AlMCM-41</i> , (b) Na- <i>AlMCM-41</i> , (c) K- <i>AlMCM-41</i> and (d) Cs- <i>AlMCM-41</i> . Inset of (B) shows the respective IR spectrum of the samples.....	102
Figure 6.6	Element distribution maps of (a) Li- <i>AlMCM-41</i> , (b) Na- <i>AlMCM-41</i> , (c) K- <i>AlMCM-41</i> and (d) Cs- <i>AlMCM-41</i>	105
Figure 6.7	FTIR spectra (a) before and after pyrrole adsorption on (b) Li- <i>AlMCM-41</i> , (c) Na- <i>AlMCM-41</i> , (d) K- <i>AlMCM-41</i> and (e) Cs- <i>AlMCM-41</i>	106
Figure 6.8	Conversion of benzaldehyde and selectivity to jasminaldehyde in aldol condensation reaction using different types of catalysts. Reaction condition: benzaldehyde:heptanal ratio = 1:5; catalyst loading = 0.25 g; temperature = 180 °C; reaction time = 60 min.	108
Figure 6.9	A proposed reaction mechanism of aldol condensation between (a) benzaldehyde and heptanal, and (b) heptanal and heptanal in the presence of <i>AlMCM-41</i> containing Li, Na, K or Cs extraframework cation solid base catalyst.....	112
Figure 7.1	Plots of degree of crystallinity versus heating time: (a) LiNKX-2, (b) NaNKX-2, (c) KNKX-2 and (d) CsNKX-2.....	116
Figure 7.2	XRD patterns of fully crystalline (a) LiNKX-2, (b) NaNKX-2, (c) KNKX-2 and (d) CsNKX-2. The crystals were obtained after 8 h, 4 h, 3 h and 2 h, respectively.	117
Figure 7.3	Proposed framework structure of M-NKX-2 aluminophosphites. Purple: Li, Na, K or Cs, red: O, pink: Al, orang: P and cyan: H.	118
Figure 7.4	SEM images of fully crystalline (a, b) Li-NKX-2, (c, d) Na-NKX-2, (e, f) K-NKX-2 and (g, h) Cs-NKX-2 at different magnifications.....	120
Figure 7.5	IR spectra of (a) LiNKX-2, (b) NaNKX-2, (c) KNKX-2 and (d)CsNKX-2.....	121
Figure 7.6	(A) ²⁷ Al and (B) ³¹ P MAS NMR spectra of (a) LiNKX-2, (b) NaNKX-2, (c) KNKX-2 and (d) CsNKX-2. Asterisks (*) denote spinning sidebands.	123
Figure 7.7	Element distribution map (SEM/EDX) of (a) LiNKX-2, (b) NaNKX-2, (c) KNKX-2 and (d) CsNKX-2.....	125

Figure 7.8	Conversion of heptanal at various reaction times using (a) LiNKX-2, (b) NaNKX-2, (c) KNKX-2 and (d) CsNKX-2 catalysts. At 180 ⁰ C for 10, 20, 30, 40, 50, 60 and 70 min.	127
Figure 7.9	Selectivity to jasminaldehyde at various reaction times using (a) LiNKX-2, (b) NaNKX-2, (c) KNKX-2 and (d) CsNKX-2 catalysts. At 180 ⁰ C for 10, 20, 30, 40, 50, 60 and 70 min.	127
Figure 7.10	Aldol reaction of benzaldehyde and heptanal using CsNKX-2 catalyst at (a) 150 °C, (b) 160 °C, (c) 170 °C and (d) 180 °C.	129
Figure 7.11	Effect of benzaldehyde and heptanal molar ratio on aldol condensation reaction based on the conversion and the selectivity to jasminaldehyde.	130
Figure 7.12	Comparative catalyst study for the aldol condensation of benzaldehyde and heptanal	131
Figure 7.13	Catalyst reusability study of Cs-NKX-2.	132

LIST SYMBOLS AND NOMENCLATURES

$^{\circ}\text{C}$	Degree Celsius
Al	Aluminum
Å	Angstrom (1×10^{-10} m)
AlO_4	Aluminum tetraoxide
AlO_5	Aluminum pentaoxide
AlO_6	Aluminum octaoxide
$\text{Al}(\text{OH})_3$	Aluminum hydroxide
AlPO	Aluminophosphate
$\text{CsOH} \cdot \text{H}_2\text{O}$	Cesium hydroxide monohydrate
HCl	Hydrochloric acid
H_3PO_3	Phosphorous acid
KBr	Potassium bromide
KOH	Potassium hydroxide
LiOH	Lithium hydroxide
M	Molarity
NaOH	Sodium hydroxide
NH_4OH	Ammonium hydroxide
nm	Nanometer (1×10^{-9} m)
O_2	Oxygen molecule
OH^-	Hydroxide ion
P_2O_5	Phosphorus pentoxide
Si	Silicon
SiO_2	Silicon dioxide
SiO_3^{2-}	Silicate
SiO_4	Silicon tetraoxide

LIST OF ABBREVIATIONS

BET	Brunauer-Emmet-Teller
ca.	Circa
FESEM	Field emission scanning electron microscopy
FTIR	Fourier transform infrared spectroscopy
HRTEM	High resolution transmission electron microscopy
h	Hour
IZA-SC	International Zeolite Association Structure Commission
MAS NMR	Magic angle spinning nuclear magnetic resonance spectroscopy
MCM-41	Mobile Composite of Material Number 41
mg	Milligram
min	Minute
NKX-2	Nankai Number 2
PP	Polypropylene
ppm	Part per million
S_{BET}	BET surface area
SAED	Selected area electron diffraction
SDAs	Structure-directing agents
TEOS	Tetraethylorthosilicate
TGA/DTA	Thermogravimetric and differential thermal analysis
TMA	Tetramethylammonium
TPA	Tetrapropylammonium
wt%	Weight percentage
XRD	X-ray diffraction
XRF	X-ray fluorescence
V_{total}	Total pore volume

**BAHAN BERLIANG MIKRO DAN MESO: KAJIAN PEMBENTUKAN,
PENCIRIAN SIFAT DAN KELAKUAN PEMANGKINAN DALAM
KONDENSASI ALDOL HEPTANAL DENGAN BENZALDEHID**

ABSTRAK

Bahan berliang memainkan peranan yang ketara dalam bidang pemangkinan, khususnya dalam sintesis bahan kimia berguna seperti jasminaldehid. Objektif projek ini adalah untuk mensintesis bahan zeolit berliang mikro dan meso sebagai mangkin aktif untuk mensintesis jasminaldehid melalui kondensasi aldol benzaldehid dengan heptanal. Bahan Komposit Mobil Nombor 41 (MCM-41) aluminosilikat berliang meso dan Nankai Nombor 2 (NKX-2) aluminofosfit berliang mikro telah dipilih dan disediakan sementara pembentukan dan sifat kedua-dua bahan juga dikaji. Pertama, pembentukan AIMCM-41 yang mengandungi kation Cs^+ (Cs-AIMCM-41) dengan morfologi nanosfera berongga yang baharu diselidik menggunakan pelbagai instrumen spektroskopi, mikroskopi dan analisis. Kemudian, kesan penggantian isomorfus Al dan penambahan hidroksida logam alkali (LiOH, NaOH, KOH dan CsOH) sebagai pemineral pada pembentukan, morfologi dan sifat permukaan MCM-41 dan NKX-2 dikaji. Penelitian menunjukkan bahawa banyak sifat pepejal berliang seperti keliangan (saiz liang, isi padu keliangan), luas permukaan, morfologi, saiz zarah dan kebesan permukaan dipengaruhi oleh pemasukan kimia Al dan jenis pemineral yang digunakan. Akhir sekali, keaktifan mangkin baharu MCM-41 mesoliang dan NKX-2 mikroliang diuji dalam tindak balas aldol antara benzaldehid dan heptanal menggunakan pemanasan gelombang mikro dan pemanasan segera bukan gelombang mikro pada 120-180 °C. Kesan parameter bagi tindak balas pemangkinan seperti jenis mangkin (pepejal MCM-41 dan NKX-2), suhu tindak balas,

masa pemanasan, jisim mangkin, nisbah reaktan dan jenis pelarut yang digunakan akan dikaji secara terperinci. Antara mangkin pepejal bes MCM-41 yang disediakan, Cs- AlMCM-41 dengan nisbah $\text{SiO}_2/\text{Al}_2\text{O}_3$ bersamaan 20 (CsM-20) mempunyai kelakuan pemangkinan yang terbaik (74.8% penukaran, 72.3% kepilihan kepada jasminaldehid) pada 180 °C dalam 60 min, diikuti masing-masing dengan CsM-5 (79.2%, 67.2%), CsM-30 (62.8%, 65.4%), K-AlMCM-41 (56.4%, 78.1%), Na-AlMCM-41 (47.3%, 75.2%), Li-AlMCM-41 (34.1%, 70.1%) dan CsM- ∞ (29.4%, 53.1%). Bagi Me-NKX-2 yang mengandungi logam, Cs-NKX-2 menunjukkan kelakuan pemangkinan yang paling bagus (87.7% penukaran, 85.2% kepilihan kepada jasminaldehid), diikuti dengan K-NKX-2 (67.8%, 70.3%), Na-NKX-2 (58.4%, 56.5%) dan Li-NKX-2 (21.9%, 32.5%). Akhirnya, mekanisme tindak balas pemangkinan aldol antara benzaldehid dan heptanal juga dicadangkan.

**MICROPOROUS AND MESOPOROUS MATERIALS: FORMATION
STUDY, PROPERTIES INVESTIGATION AND CATALYTIC BEHAVIOR
IN ALDOL CONDENSATION OF HEPTANAL AND BENZALDEHYDE**

ABSTRACT

Porous materials play a significant role in the area of catalysis, particularly in the synthesis of useful chemicals such as jasminaldehyde. The objectives of this project are to synthesize microporous and mesoporous zeolite materials as active catalysts for synthesizing jasminaldehyde *via* aldol condensation of benzaldehyde with heptanal. Mesoporous aluminosilicate Mobil Composite Material number 41 (MCM-41) and microporous aluminophosphate Nankai Number 2 (NKX-2) are chosen and prepared while the formation and the properties of both materials are also studied. Firstly, the formation of AlMCM-41 containing Cs⁺ cation (Cs-AlMCM-41) with novel hollow nanosphere morphology is investigated using various spectroscopy, microscopy and other analytical instruments. Then, the effects of isomorphous Al substitution and the addition of alkali metal hydroxides (LiOH, NaOH, KOH and CsOH) as mineralizers on the formation, morphological and surface properties of MCM-41 and NKX-2 are also investigated. The results show that many properties of the porous solids such as porosity (pore size, pore volume), surface area, morphology, particle size and surface basicity are significantly affected by the chemical incorporation of Al and the use of different types of mineralizers. Lastly, the catalytic activity of mesoporous MCM-41 and microporous NKX-2 novel catalysts are tested in aldol reaction between benzaldehyde and heptanal using microwave and non-microwave instant heatings at 120-180 °C. The effects of catalytic reaction parameters such as type of catalyst used (MCM-41 and NKX-2 solids), reaction temperature,

heating time, catalyst loading, reactants ratio and type of solvent used are studied in detail. Among all the MCM-41 solid base catalysts prepared, Cs- AIMCM-41 with $\text{SiO}_2/\text{Al}_2\text{O}_3$ ratio of 20 (CsM-20) had the best catalytic performance (74.8% conversion, 72.3% selective to jasminaldehyde) at 180 °C for 60 min, followed by CsM-5 (79.2%, 67.2%), CsM-30 (62.8%, 65.4%), K- AIMCM-41 (54.4%, 78.1%), Na- AIMCM-41 (47.3%, 75.1%), Li- AIMCM-41 (34.1%, 70.1%) and CsM- ∞ (29.4%, 53.1%), respectively. For metal incorporated Me-NKX-2, Cs-NKX-2 showed the best catalytic performance (87.7% conversion, 85.2% selective to jasminaldehyde), followed by K-NKX-2 (67.87%, 70.23%), Na-NKX-2 (58.4%, 56.5%) and Li-NKX-2 (21.97%, 32.5%). Finally, the catalytic reaction mechanism of aldol reaction between benzaldehyde and heptanal is also proposed.

CHAPTER ONE

INTRODUCTION

1.1 General introduction

Porous materials plays a significant role in the area of material chemistry. These materials have largely been utilized in catalysis, ion exchange, separation and adsorption due to their unique properties, including uniform pore sizes, high surface areas and tunable framework structures (Chawla et al., 2018; Xiaoyun et al., 2013; Koohsaryan 2016). According to the International Union of Pure and Applied Chemistry (IUPAC), porous solid can be classified into three groups, namely micropores: $\text{\AA} < 2.0$ nm, mesopores: $\text{\AA} = 2\text{-}50$ nm, and macropores: $\text{\AA} > 50$ nm, where \AA is the pore diameter (Moshoesheoe et al., 2017). Amid the porous solids, aluminosilicate, aluminophosphate, aluminophosphite zeolites and metal organic frameworks (MOFs) fall in the microporous category whereas other mesoporous materials like Mobil Composite Material number 41 (MCM-41) and number 48 (MCM-48), and Santa Barbara Amorphous number 15 (SBA-15) fall in the mesoporous category (Wong et al., 2018).

In general, zeolite materials are prepared in protonated form as they are usually employed as solid acid catalysts in refining and petrochemistry industries (Spangsberg et al., 2011). Recently, design and preparation of solid base catalysts are getting more attentions particularly in the preparation of fine and expensive chemicals considering their unique properties as compared to the homogeneous liquid base catalysts. Their marvellous properties including large pore size and high shape selectivity, which go along with the possibilities for having strong basicity and high reusability (Maghsoodloorad et al., 2011).

Jasminaldehyde (α -pentylcinnamaldehyde) is an important chemical of commercial interest due to its perfumery, pharmaceutical and medical applications. This compound is synthesized and consumed in Europe in 100 tonnes annually (Api et al., 2015). The production of jasminaldehyde in the U.S is reported between 230 kg and 450 kg in 1990. The production increased to 4.50 tons in 2000s and above 1000 metric ton in 2011 (Api et al., 2016). The market price for jasminaldehyde ranging from US\$4.70-5.00 per kilogram. Typically, jasminaldehyde is produced *via* aldol condensation of heptanal and benzaldehyde where stoichiometric amount of NaOH or KOH homogeneous catalyst is used (Gopal et al, 2001). The pronounce problems of the homogeneous catalytic process for synthesizing jasminaldehyde are poor recyclability, generation of large amount of corrosive waste, use of harmful homogeneous catalysts and requirement of post treatment of spent liquid effluent which increases the operation cost.

In order to avoid such problems, hydrotalcites, rare earth alkali metal oxides, alkali metal exchanged and impregnated solid supports (e.g. zeolites) have been designed and used as heterogeneous solid base catalysts (Koekkoek et al, 2011; Weckhuysen et al., 2014; Gopal et al., 2016; Weitkamp et al., 2001; Xie et al., 2009; Rodriguez et al., 1999). These solid base catalysts are found to be reactive in many catalytic reactions, such as aldol condensation, self-condensation of acetone, Knoevenagel condensation, etc. (Parida et al, 2009; Kleotstra at al., 1997; Yu et al., 2003; Fan 2019).

1.2 Development of zeotype solid base catalysts

The use of zeolites as base catalysts started in early 1990's where the catalysts are prepared in ion ex-change form (Michalska et al., 2004). Since then, impregnation

of zeolites with various alkali salts is reported with the aim to produce much stronger basic sites in zeolite frameworks (Venkatesan et al., 2005). However, the small pore size of zeolite materials (ca. 5.0 Å for 10-membered ring zeolites) has restricted their applications in synthesizing fine chemicals involving bulk molecules as the small pore opening of zeolites prevents the bulky molecules from diffusing into the micropores and reaching to the active site of the catalysts (Shang et al., 2011). To overcome the pore size constraint, MCM-41 mesoporous solids which has larger pore diameter (ca. 20-30 Å) has been fabricated. Process such as impregnation, ion-exchange and direct (one-pot) synthesis of basic MCM-41 are explored (Lin et al., 1999; Sharma et al., 2010; Martins et al., 2010; Wiesfelf et al., 2017). For instance, cesium acetate has been impregnated on MCM-41 followed by calcination (Martins et al., 2010; Wiesfelf et al., 2017). An excellent dispersion of cesium oxide cluster is observed in the mesopores where the cesium oxide clusters are active in Knoevenagel condensation and Michael addition reactions.

Furthermore, another interesting approach for preparing MCM-41 solid base catalyst by anchoring organic bases (e.g. amines) on the silanol groups of MCM-41 is reported (Dartt and Davis, 1994; Putz et al., 2015; Murugavel et al., 2008). This functionalization technique ensures the chemical connection between the inorganic host and the organic base species *via* covalent bonds (e.g. (3-aminopropyl)triethoxysilane) while low leaching of functionalized species is expected. In addition, the functionalized MCM-41 solid base catalyst can also be prepared by reacting the Si-OH groups with 3-trimethoxysilylpropyl(trimethyl)ammonium chloride and then followed by ion exchange with Cl⁻ and OH⁻ anions (Gan et al., 2015). Although these organo-functionalized MCM-41 catalysts are interesting due to their good catalytic performance and low leaching issue, they still possess several

drawbacks. First, the synthesis procedure is complicated where it involves multiple steps of preparation. Second, the organosilanes are expensive, and third, the resulting catalysts can only be used in the mild catalytic reaction condition ($<170\text{ }^{\circ}\text{C}$) because the organosilanes tend to degrade at high temperature. Hence, the solid base catalysts with simple preparation, cheap, non-toxic, catalytically active, high selective and reusable are highly desired.

One pot synthesis of solid base catalysts is interesting since it is simple, and it meets all the requirements stated above. This technique can be achieved *via* hydrothermal synthesis of zeolite materials where mineralizers with different basicities (to increase their basic strengths), and isomorphous substituted heteroatoms such as Al, B and Ga (to increase the basic active sites) are added during the synthesis. However, this approach is rarely reported because the catalytic activity of the prepared catalysts is low especially under normal reflux conditions.

1.3 Aims of the study

In this work, it is aimed to enhance the catalytic performance of the synthesis of jasminaldehyde by searching potential solid base catalysts and employing appropriate reaction conditions. For the zeolite catalysts studied, the materials must be easy to prepare, cheap, non-toxic, catalytically active, high selective to jasminaldehyde and reusable. Two types of solid base catalysts, namely aluminosilicate mesoporous MCM-41 (pore size ca. 20 \AA) and large-microporous NKX-2 aluminophosphate (pore size ca. 7 \AA) zeolites, have been identified where their large pores allow the diffusion of benzaldehyde ($4.9 \times 4.3 \times 1.9\text{ \AA}^3$), heptanal ($9.7 \times 2.0 \times 1.8\text{ \AA}^3$) and jasminaldehyde ($6.9 \times 9.2 \times 1.8\text{ \AA}^3$) (*Hyper Chem 7.0* software). For MCM-41 solid base catalyst, it is obtained through isomorphous substitution of Al into the MCM-41 framework *via*

direct (one-pot) hydrothermal synthesis route. In addition, metal hydroxides such as LiOH, NaOH, KOH and CsOH are also added as mineralizers. The effects of Al loading and the mineralizers on the formation, properties and catalytic performance of prepared MCM-41 mesoporous materials in aldol condensation reaction between heptanal and benzaldehyde were investigated. Furthermore, an attention is also given to the synthesis of large-microporous NKX-2 aluminophosphate base catalyst where the previous works reported that this solid synthesized using organic template has weak basicity due to the absence of basic sites (Li et al., 2006). In the present work, NKX-2 containing different alkali metal extra-framework cations are prepared using simple organotemplate-free hydrothermal route where H_3PO_3 is used as a phosphorus initial source. In addition, the effects of mineralizers on the formation, properties and catalytic activity of the prepared alkali metal containing NKX-2 in the synthesis of jasminaldehyde are investigated. For the catalytic reaction study, novel heating methods, namely microwave heating and non-microwave instant heating are applied. The first method provides fast and homogeneous heating whereby the heat is generated *via* molecular rotation mechanism after microwave radiation is absorbed, while the latter one is also able to provide fast and homogenous heating as microwave heating but using other heating mechanism, namely very fast stirring and very fast heating rate.

1.4 Objectives of the study

- a. To perform time-dependent study on the formation and morphology of Cs- AlMCM-41 .
- b. To investigate the effects of Al content on the formation, properties and catalytic behavior of Cs- AlMCM-41 in aldol condensation of benzaldehyde and heptanal.

- c. To explore the effects of mineralizers (LiOH, NaOH, KOH and CsOH) on the formation, properties and catalytic behavior of prepared AlMCM-41 solids in aldol condensation of benzaldehyde and heptanal.
- d. To investigate the effects of various alkali metal cations (Li^+ , Na^+ , K^+ and Cs^+) on the formation of NKX-2, and their catalytic performance in aldol condensation of benzaldehyde and heptanal.

1.5 Scope of the thesis

This thesis comprises of eight chapters. Chapter One is dedicated to the general introduction, classification of microporous, mesoporous and macroporous materials, brief history of solid base catalysts and jasminaldehyde. Chapter Two is a comprehensive literature review describing the history, synthesis and properties of microporous and mesoporous materials (NKX-2 and MCM-41) together with their fundamental concept of formations. Furthermore, a description about the characterization techniques used in this study is also mentioned in this chapter.

Chapter Three presents the experimental methodology used in this study where the preparation of Me-AlMCM-41 (Me = Li, Na, K or Cs), formation study of Cs-AlMCM-41 and Me-NKX-2 (Me = Li, Na, K, or Cs) materials *via* hydrothermal approach are comprehensively described. Furthermore, the information on the analysis set-up for characterization of samples, such as X-ray diffraction analysis (XRD), thermogravimetry and differential thermal gravimetry analysis (TG/DTG), Fourier transform infrared spectroscopy (FT-IR), nitrogen sorption isotherm analysis, solid state nuclear magnetic resonance spectroscopy (^{27}Al , ^{29}Si and ^{31}P MAS NMR), field emission scanning electron microscopy (FESEM), energy-dispersive X-ray spectroscopy (EDX), inductively coupled plasma atomic emission spectroscopy (ICP-

OES), X-ray fluorescence spectroscopy (XRF), nitrogen adsorption analysis, temperature program desorption (TPD-CO₂) analysis, gas chromatography (GC), and gas chromatograph-mass spectrometry (GC-MS), are also detailed in this chapter.

Chapter Four describes an investigation of the formation of Cs-*AlMCM-41* with novel hollow nanosphere morphology. The synthesis is conducted using hydrothermal approach and the evolution of the formation of Cs-*AlMCM-41* hollow nanospheres is periodically monitored. Chapter Five is dedicated to the study of the effects of Al addition on the physicochemical and catalytic properties of ultrasmall Cs-*AlMCM-41* solids. Then, the catalytic behavior of this solid in the synthesis of jasminaldehyde under microwave-assisted condition is evaluated.

Chapter Six presents the mineralizer (Me = LiOH, NaOH, KOH and CsOH) effects on the physicochemical and catalytic properties of Me-*AlMCM-41* mesostructured solids. Various characterization techniques are employed to reveal these effects before the catalytic properties of Me-*AlMCM-41* are tested in aldol condensation between heptanal and benzaldehyde under non-microwave instant heating condition. Then, the catalytic reaction mechanism of aldol condensation in the presence Me-*AlMCM-41* catalyst is proposed in this chapter.

In Chapter Seven, the mineralizer effects on the nucleation, crystal growth and physicochemical properties of Me-NKX-2 zeolites are discussed. LiOH, NaOH, KOH and CsOH are used as mineralizers and inorganic template where H₃PO₃ is used as a phosphorus source. Then, the catalytic performance of metal-containing NKX-2 in microwave-assisted aldol condensation reaction for synthesizing jasminaldehyde is described.

Finally, the summary of principal findings is presented in Chapter Eight. Some suggestions and recommendations for the impending work to widen the prospect and the use of MCM-41 and NKX-2 as potential solid base catalysts in fine chemical synthesis are also highlighted.

CHAPTER TWO

LITERATURE STUDY

2.1 Microporous zeolite and zeotype solids

Zeolites are microporous aluminosilicates composed of silica (SiO_4) and alumina (AlO_4) tetrahedra with O atoms connecting neighbouring tetrahedral. When the framework is made up of pure siliceous structure (SiO_4 units) in this fashion, a neutral zeolite framework is produced. However, the zeolite framework will become negatively charged after incorporation of Al in the form of tetrahedra $[\text{AlO}_4]^-$ where extra-framework inorganic cation (M^+) is needed to neutralize the negative charge so as to maintain the electrical neutrality of the framework (Figure 2.1) (Wiesfield and Hensen, 2017; Alothman, 2012).

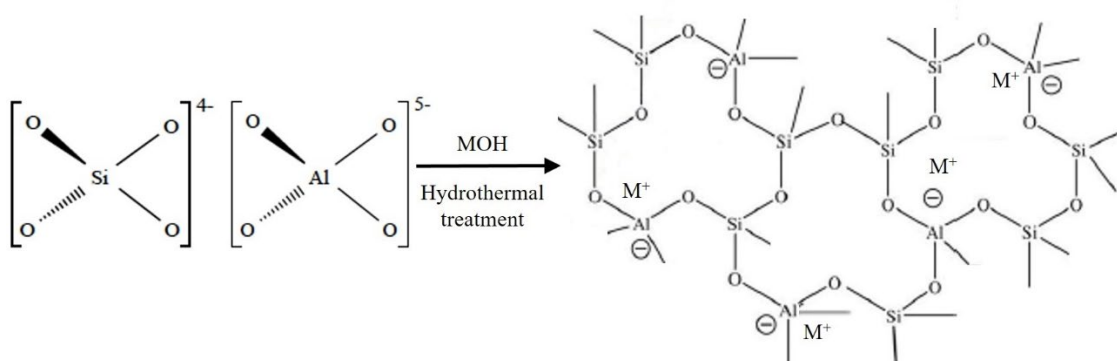


Figure 2.1. Arrangement of AlO_4 and SiO_4 tetrahedra, and metal cation ($\text{M}^+ = \text{Na}^+$ or K^+) in zeolite framework.

The zeolite composition can best be described as $\text{M}_n x/n \cdot [(\text{AlO}_2)_x (\text{SiO}_2)_y] \cdot w\text{H}_2\text{O}$ where M is generally a group I or II element (e.g. sodium, potassium or magnesium). The variable n stands for the cation valance, x is equal or greater than 2, y is 2 to 10 and w is the amount of water molecules bound to zeolite structure.

Zeotype molecular sieves are another porous solid exhibiting identical structure as zeolites but with different elemental compositions in the framework (Zhang and Haung, 2015). Among examples of those porous solid are aluminophosphates (AlPO-n), aluminophosphites (AlPO-n), titanosilicate (TiSi), gallium phosphate (GaPO-n), MCM-41, silicoaluminophosphate (SAPO-n), germanosilicate (GeSi) and metal aluminophosphate (MeAPO-n) (Morris & Huddersman, 1999; Koch et al. 1998). All these zeolite-like materials can only be obtained synthetically, and they have been widely used as catalysts and adsorbent (Lagno and Demopoulos, 2005).

In 1980s, Wilson and his colleagues discovered AlPO-n microporous materials (n is referred to type of the structure) (Li et al., 2008). The major difference between AlPOs and zeolites is that AlPOs have neutral charge framework which contrasts with negatively charge framework of zeolite (Figure 2.2). Another difference is that the Al atom in AlPOs can exist in four, five and/or six coordination whereas the Al atoms in zeolites always exist in tetrahedral coordination (Zheng and Huang, 2015; Lagno and Demopoulos, 2005; Li et al., 2008; Venkatathri et al., 1998).

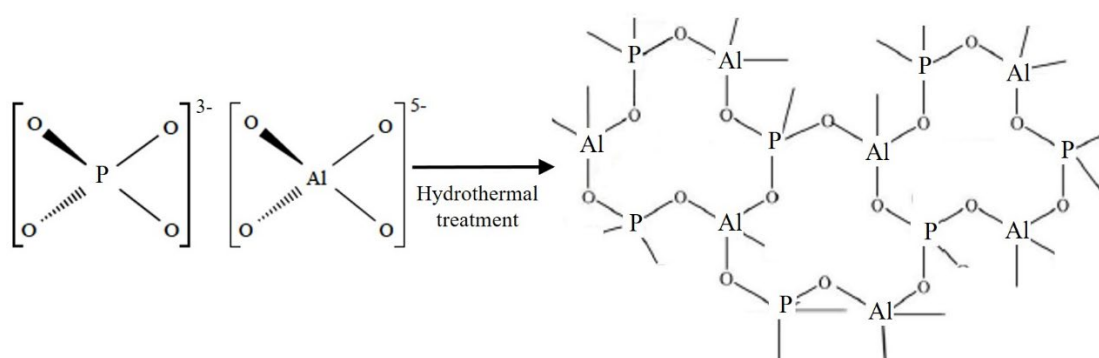


Figure 2.2. Arrangement of PO₄ and AlO₄ in AlPO zeotype framework which have neutral framework.

The open-framework AlPOs can be classified into two main groups, namely AlPOs neutral framework with Al/P ratio = 1, and AlPOs anionic framework with Al/P

ratio < 1 (Li et al., 2008). In AIPOs neutral framework, it is constantly produced by alternating AlO_4 and PO_4 tetrahedra. This usually resemble aluminosilicate zeolite framework. In addition, AIPO frameworks that are constructed by the Al-O-P bonds always follow Lowenstein's rule where the formation of Al-O-Al and P-O-P linkages in AIPO-n are forbidden. Therefore, based on this rule, the AIPO-n molecular sieves built from even-numbered rings are formed. The molecular formula of AIPO-n is generally described in the form of $[(\text{AlO}_2)_x(\text{PO}_2)_x].y\text{H}_2\text{O}$. Conversely, the AIPO molecular sieves with anionic frameworks are constructed from the combination of Al polyhedra (tetrahedral, pentahedral and octahedral Al) and tetrahedral P species (Lagno and Demopoulos, 2005; Li et al., 2008). However, terminal P-OH and P=O can be presented in the AIPO-n framework, making the framework anionic charged and Al/P ratio $\neq 1$ (Hamza and Nagaraju, 2015).

The negative charges of AIPOs are usually balanced by organic or inorganic cationic species (Chao et al., 2017). As a result, hydrogen bonding between these cationic species with P-OH and P=O groups occurs and indirectly stabilizing the framework (Chao et al., 2017). Two famous examples of this kind material are JOF-20 (Al/P = 0.77) and NKX-2 (0.72) (Hamza and Nagaraju, 2015).

2.2 Nankai Number 2 aluminophosphate (NKX-2)

Aluminophosphate (NKX-2) is a class of zeolite material, Figure 2.3. It is normally crystallized hydrothermally where phosphorus source used is phosphorous acid [42]. Phosphorous acid, H_3PO_3 , is an acid with diprotic acid ($\text{pK}_{a1} = 1.79$, $\text{pK}_{a2} = 6.14$) character, having $\text{HPO}(\text{OH})_2$ structural formula. In H_3PO_3 , $\text{HPO}(\text{OH})_2$ and $\text{P}(\text{OH})_3$ tautomers occur in equilibrium where the phosphorus appears in the form of P^{3+} [43]. H_3PO_3 is found to behave differently from H_3PO_4 during the crystallization

process of aluminophosphites and aluminophosphates. When H_3PO_3 is used as the phosphorus source, NKX-2 aluminophosphite is formed, whereas this crystalline phase is not observed in the synthesis route containing H_3PO_4 as the phosphorus source.

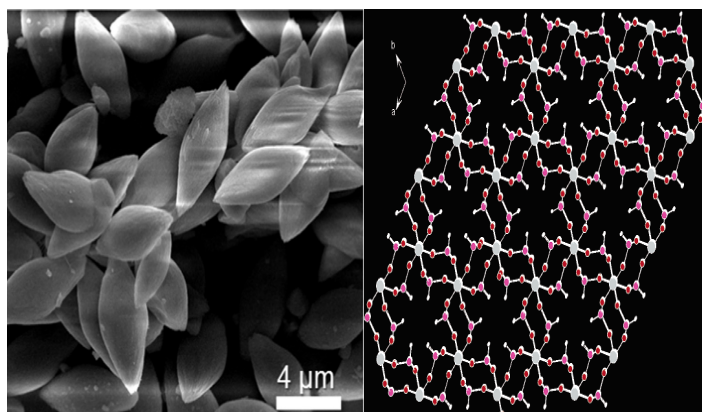


Figure 2.3. Crystal and chemical structure of NKX-2 (Gopal et al., 2016; Li et al., 2006).

In NKX-2, the P atoms exist in tetrahedral (PO_4) coordination, which is the same as aluminophosphate materials. But, the Al atoms frequently appear in octahedral coordination (AlO_6). In some occasion, the Al atoms also exist in pentahedral (AlO_5) as well tetrahedral (AlO_4) arrangements (Eng et al., 2016). The NKX-2 framework is also built up from Al-O-P bonds and the Al-O-Al arrangement might also be observed (Eng et al., 2016; Li and Xiang, 2002; Shi et al., 2014). The framework structure of NKX-2 is metastable where the transformation of NKX-2 to (silico)aluminophosphate microporous materials (e.g. AEL, FAU, AFO, ATO, AFI) has been reported as a result of the phosphorus nutrients releasing from NKX-2 that are essential for crystallizing these AlPOs (Zong et al., 2017).

2.2.1 Synthesis of NKX-2

NKX-2 can be obtained from hydrothermal method using organic templates. For example, this molecular sieve has been crystallized under hydrothermal conditions at 175-195 °C for 2-5 days using triethyl amine as organic template (Li et al., 2006; Li and Xiang, 2002). In addition, the synthesis of NKX-2 using ionothermal route is also reported recently (Yang, 2018; Eng et al., 2016). Unlike hydrothermal route, this technique uses ionic liquids as solvents and organic templates. Compared to hydrothermal heating (96 h, 160 °C), crystalline NKX-2 can be obtained within shorter period under ionothermal condition (2 h, 170 °C) (Shi et al., 2014). The NKX-2 crystals synthesized from ionothermal heating are also found to be different from those prepared using hydrothermal method due to the unique chemical properties (polarizability, solubility, ionic interaction, etc.) of the ionic liquids used. Recently, the hydrothermal synthesis of NKX-2 containing Na⁺ extraframework cation without using organic template is also reported (Gopal et al., 2016). It is shown that the synthesis time of NaNKX-2 is significantly reduced to 4 h as compared to previous works. By using NaOH as mineralizer and inorganic template, NaNKX-2 with grain-like shape is obtained and these crystals are a good catalyst in base-catalyzed cyanoethylation of methanol.

2.3 MCM-41 mesoporous molecular sieves

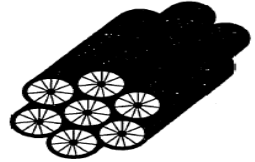
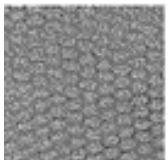
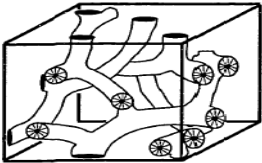
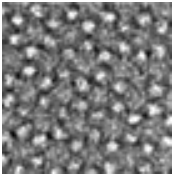
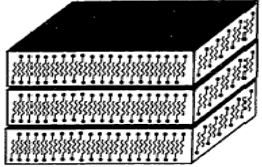
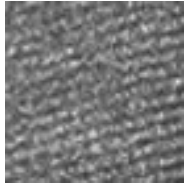
In 1992, Mobil Oil Inc. has successfully synthesized a new class of material named M41S (Matei et al., 2016). This breakthrough has made the molecular sieve industry bloom owing to their unique properties having a uniform pore size in mesoporous range (20-100 Å). Thus, the pore size limitation faced by zeolite microporous solids (pore size <20 Å) has been overcome.

M41s material consists of three analogue materials (Table 2.1). The MCM-41 displays 2-D hexagonal arrangement of porous silica, while MCM-48 has cubical arrangement and a 3-D pore system, and lastly MCM-50 has lamellar arrangement. The research efforts have been focused on MCM-41, as it is relatively more thermally stable and easier to obtain. Furthermore, it has more superior adsorption and surface properties than its counterparts (Wang et al., 2006; Rath et al., 2014; Mokri et al., 2019; Kresge et al., 1992; Alotman, 2012).

Typically, MCM-41 (Mobil Composite Material number 41) is the most useful analogue among the M41s members. It has superior (hydro)thermal stability which can withstand a temperature until 815 °C. In addition, it is comparatively stable in acid solution (pH 2.5) (Ghomari et al., 2015). Nevertheless, the mesostructure is not stable in high basic medium (above pH 12). Pure siliceous MCM-41 is almost catalytically inactive as a result of its electrical neutrality. Consequently, the isomorphous insertion of Si with various metals (Al, Ga, Fe) is needed to give rise to acid or base property (Das et al., 1999; Tuel, 1999). In addition, the feasibility of using the mesopores of MCM-41 to act as a catalyst support is also widely studied (Bhattacharyya and Saboungi, 2006; (Bhattacharyya and Soboungi, 2006; Xie et al., 2009; Rodriguez et al., 1999).

Table 2.1

Members of M41s mesoporous materials (Murugavel et al, 2008; Alothman, 2012).

Analogue	Phase	Possible structure	Morphology	Properties
MCM-41	Hexagonal			<ul style="list-style-type: none">• Highly ordered mesoporosity• 2D channel system• High surface area (800 m² g⁻¹)• High (hydro)thermal stability (max. 815 °C)• Acidic/basic character depends on treatments
MCM-48	Cubic			<ul style="list-style-type: none">• Highly ordered mesoporosity• 3D channel system• Large surface area (1028 m² g⁻¹)• High (hydro)thermal stability (max. 750 °C)• Acidic/basic character depends on treatments
MCM-50	Lamellar			<ul style="list-style-type: none">• Highly ordered mesoporosity• 2D channel system• Large surface area (800 m² g⁻¹)• Mild (hydro)thermal stability (max. 550 °C)• Acidic/basic character depends on treatments

2.3.1 Synthesis and formation of MCM-41

The synthesis of MCM-41 mesoporous material requires four ingredients, namely silica source (basic framework units), organic template (as pore directing agent), mineralizing agent (to solubilize silica) and solvent (to assist mass and heat transfers). The silica sources are either colloidal silica or organic silicon alkoxides that are soluble in water while sodium hydroxide or concentrated ammonia are as mineralizers. The templates are the quaternary ammonium halides having long alkyl chain length (e.g. cetyltrimethylammonium bromide or CTABr) where the template has hydrophobic tail and hydrophilic head (Parida and Rath, 2009; Kloestra et al., 1997).

The conventional pathway of the formation of MCM-41 is *via* liquid crystal templating (LCT) process (Bagshaw and Bruce, 2008). In the path of synthesis route, the CTA⁺ ions agglomerate to form spherical micelles to avoid repulsion. Usually, the micelle in spherical shape is unstable due to its high Gibbs free energy, and hence the spherical micelles prefer to form a micelle cluster with rod-like shape which is more thermodynamically stable. Further combination of the rod shape micelles forms closely packed structure with hexagonal array. The silicate monomers and oligomers then further interact with the micelles and polycondense at the interface of micelles, forming MCM-41 material as precipitated solid. The amorphous nature of MCM-41 is concealed due to possessing of the long-range ordered arrangement (Xie et al., 2009). This give the characteristic XRD peaks at low 2θ when it is subjected to X-ray diffraction measurement (Rodriguez et al., 1999). In order to open the pores of MCM-41, high temperature calcination (500-600 °C) or solvent extraction treatment (i.e. acidic ethanol solution) is applied (Figure 2.4) (Xie et al., 2009; Rodriguez et al., 1999;

Parida and Rath, 2009; Kloestra et al., 1997; Bagshaw and Bruce, 2008; Michalska et al., 2004; Vekatesan et al., 2011).

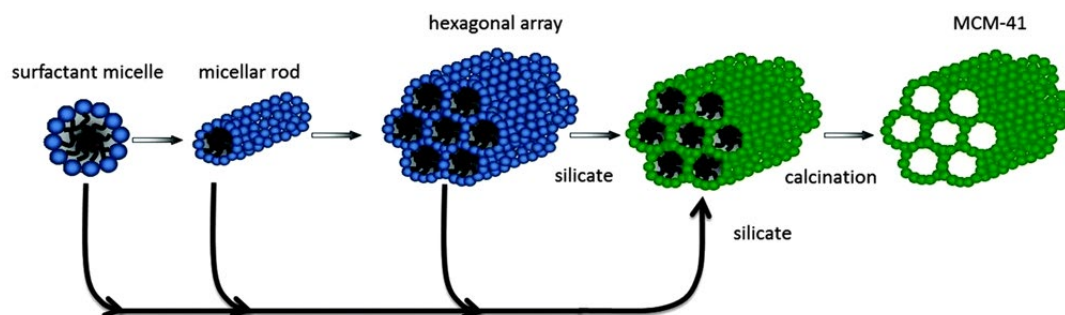


Figure 2.4. Formation of MCM-41 *via* liquid crystal templating mechanism (Althman, 2012).

2.3.2 Generation of catalytic active sites on MCM-41

Pure silica mesoporous material has no acidity/basicity. Hence, several strategies have been introduced to generate solid acidity/basicity. For instance, the insertion of metals such as Al, Ti, Ga and Zr into the mesostructural framework has been reported (Shang et al., 2011).

The acidities (Brönsted and Lewis acids) generated is normally associated with the presence of heteroatoms (e.g. aluminum) in the framework (Figure 2.5) (Rodriguez et al., 1999). The aluminum containing MCM-41 materials can be engineered by using both direct and post synthesis methods. The formation of mesopores with desired size openings can also be performed by simply adjusting the alkyl chain length of the surfactant (Lin et al., 1999).

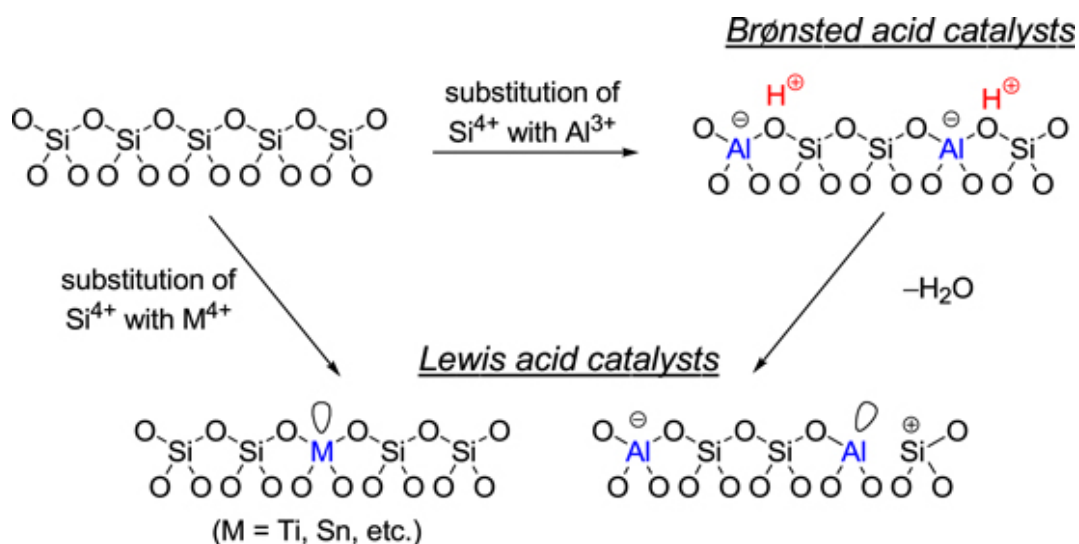


Figure 2.5. Formation of Brønsted and Lewis acid sites in MCM-41 framework by isomorphous substitution of Al or other heteroatoms.

On the other hand, the basicity of molecular sieves can be achieved by exchanging the extraframework cations, which counterbalance the negative charge developed by aluminum atom in the framework (Figure 2.6) (Lin et al., 1999). Normally, highly electropositive cations such as Cs⁺, K⁺, Ca²⁺, Mg²⁺ and Ba²⁺ are excellent candidates to be exchanged and to prepare solid base catalysts. Besides that, the surface basicity of zeolite materials can also be generated by depositing the solid metallic oxides (e.g. Cs₂O, CaO, MgO, K₂O) that possess strong basic characteristics to the mesoporous material (Lin et al., 1999). Solid base MCM-41 catalyst can also be synthesized *via* grafting or anchoring organosilanes containing base functionality (e.g. amines) (Figure 2.7) (Martins et al., 2010). This method can be done through covalently bonding the organosilane on the surface silanol under mild temperature and reflux conditions.

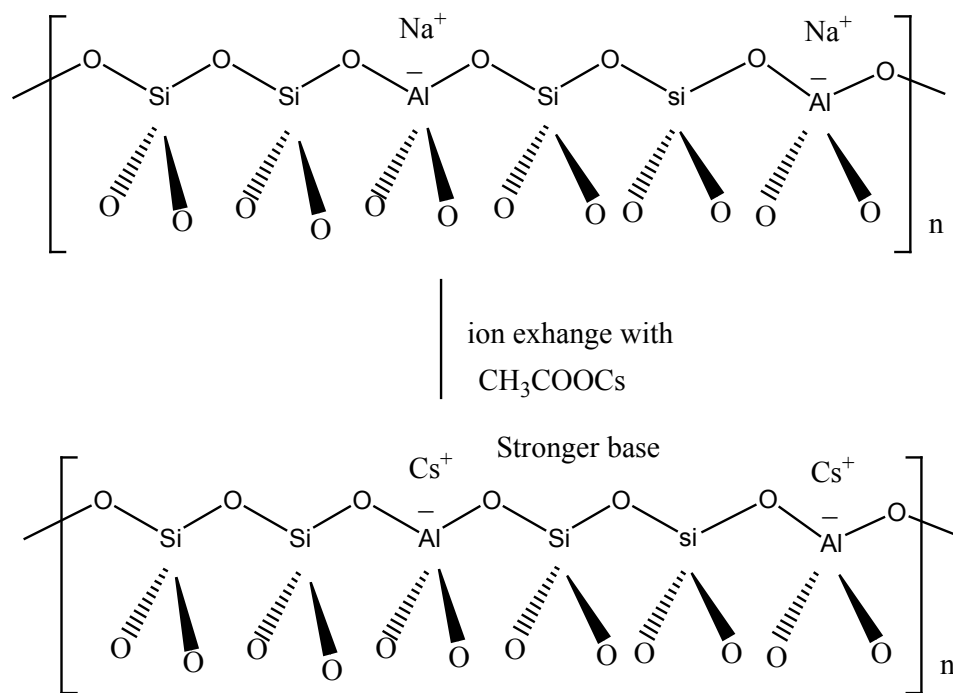


Figure 2.6. Preparation of highly basic Cs- AlMCM-41 via ion exchange of Na-AlMCM-41 using cesium acetate.

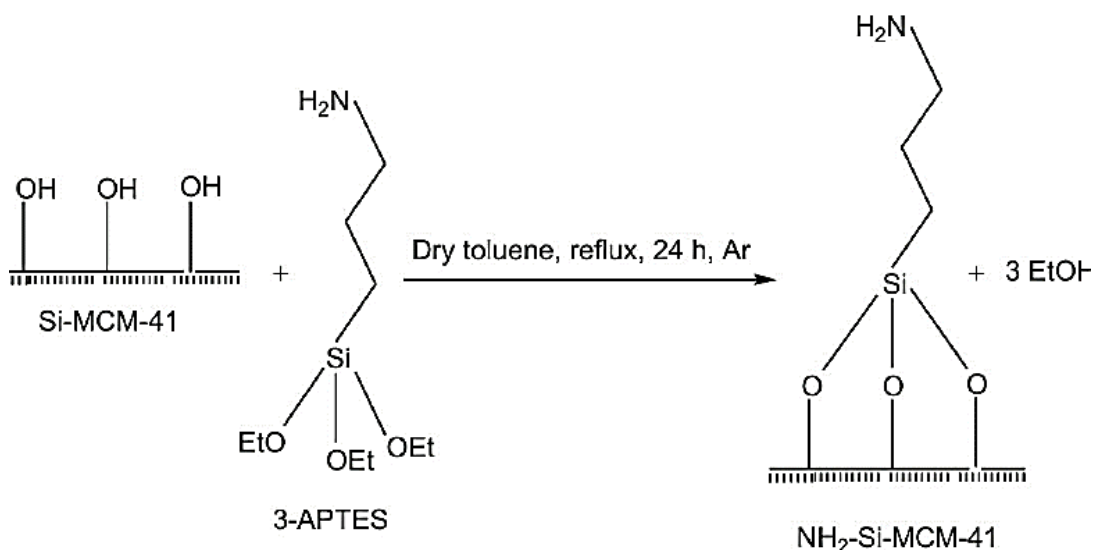


Figure 2.7. Generation of basic sites by functionalization of organosilane such as 3-aminopropyltriethoxysilane onto the surface of MCM-41 (Monnier et al., 1993).

2.4. Synthesis of jasminaldehyde *via* catalytic aldol condensation between benzaldehyde and heptanal

Jasminaldehyde or α -pentylcinnamaldehyde is a well-known perfume ingredient with an aromatic scent. It is used extensively in perfumery industries. Jasminaldehyde is usually synthesized *via* aldol condensation between benzaldehyde and heptanal catalyzed in both acidic and basic media (Figure 2.8) (Naik et al., 2003). Traditionally, it is prepared using homogeneous bases (i.e. KOH, NaOH) in more than stoichiometry. Recently, the heterogenous solid bases take the center stage due to several problems faced by homogeneous catalysis system such as severe environmental concern in waste disposal, toxic, difficulty of handling and storing corrosive homogeneous catalysts, difficulty in separation and recycling problem. Many solid base catalysts used to synthesize jasminaldehyde with high selectivity have been reported.

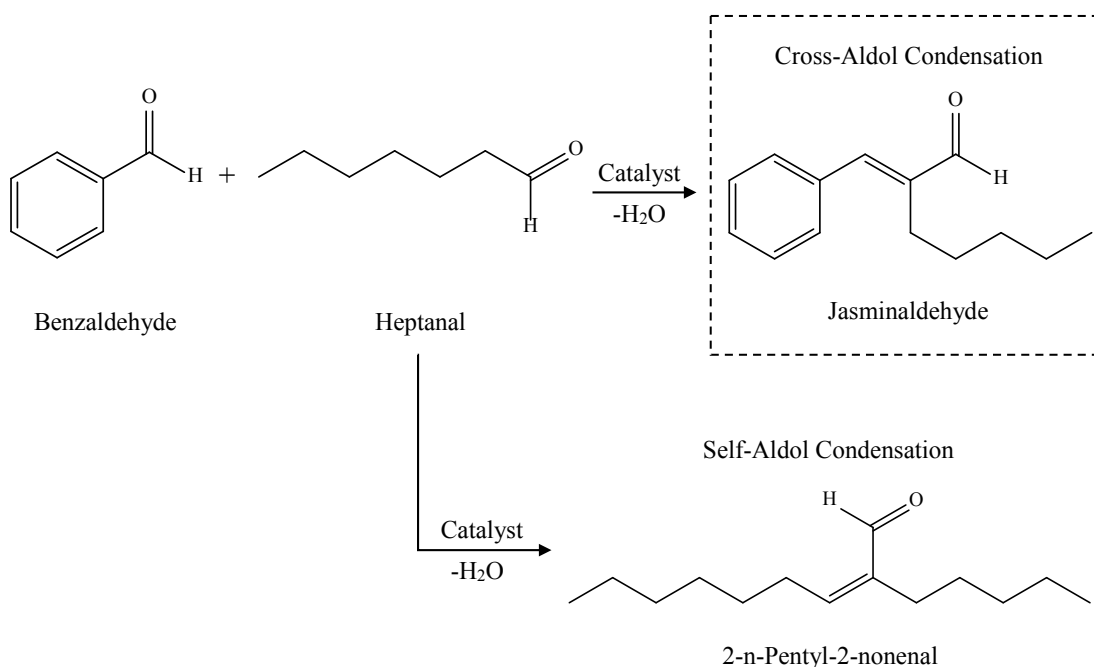


Figure 2.8. Synthesis of jasminaldehyde using aldol condensation of benzaldehyde and heptanal.

Clement et al. observed that in aldol condensation reaction involve benzaldehyde and heptanal recorded low selectivity to jasminaldehyde when using microporous zeolite as catalyst (Martins et al., 2010). The smaller pore size of the zeolite coupled with the larger molecule size of both the reactant and the product cause rapid deactivation of catalyst due to trap molecule in microporous zeolite void. Therefore, the formation of 2-pentyl-2-nonenal and diphenyl allyl cation take center stage as the product of self-aldol condensation of heptanal and benzaldehyde, respectively. On the other hand, the use of mesoporous aluminosilicate (AIMCM-41) gave an excellent catalytic performance and selectivity to jasminaldehyde than using microporous zeolites. AlPO-n zeotype catalyst also displayed an excellent performant as catalyst and appeared as the best catalyst among the catalyst tested. The whole idea attributed to the acid-base bifunctional character of the aluminophosphate. Hence, the benzaldehyde molecule was activated by weak acid sites *via* protonation of the carbonyl functional group. This will in turn facilitate the attack of heptanal intermediate (enolate) produce from weak basic site of the amorphous aluminophosphate catalyst.

Sudheesh et al. found that the polymeric chitosan catalyst is very pronouns and highly performed catalyst in jasminaldehyde synthesis with reasonable selectivity to jasminaldehyde through aldol condensation of heptanal and benzaldehyde (Sudheesh et al., 2010). They reported about >99% conversion of heptanal with 88% selectivity to jasminaldehyde were achieved under solvent free condition at 160 °C for 8 h with 100 mg catalyst loading. The study further evaluates other reaction parameters which include catalyst amount, temperature and heptanal to benzaldehyde ratio. As expected, the increase in temperature and catalyst amount significantly affect the heptanal

conversion and the selectivity to jasminaldehyde. The catalyst performance was preserved up to the six cycles.

Patil et al. worked on novel double metal cyanide. The composite is a powerful bifunctional catalyst with strong Lewis basic side from the cyanide and Lewis acid side from the empty orbital of the double metals ion site. The catalyst performed effectively in solvent free synthesis of jasminaldehyde *via* aldol condensation reaction of heptanal with benzaldehyde (Patil et al., 2013). Also, the composite catalysts having Fe^{2+} and Zn^{2+} with complexing agents also displayed high activity for the synthesis of jasminaldehyde (93% conversion, 77% selectivity to jasminaldehyde) at 170 °C for 12 h. It was speculated that Fe^{2+} and Zn^{2+} cations contained free orbital and act as Lewis acid which can easily activate the carbonyl functional group of benzaldehyde.

Sharma et al. designed and prepared hydrotalcite catalyst material for synthesizing jasminaldehyde. The selectivity to jasminaldehyde increased significantly when Mg/Al molar ratio increased (Sharma et al., 2010). The MgO presumed to be the active basic site of the composite. For the as-synthesized sample with 3.5 molar ratio, the conversion of heptanal reached up to 98% with 86% selectivity to jasminaldehyde. However, thermally activated hydrotalcite was more active for self-condensation of heptanal compared to the cross-aldol condensation of heptanal and benzaldehyde. The catalyst loading significantly affected the conversion of heptanal and selectivity to jasminaldehyde. They also observed the reaction conversion increased when more catalyst loading was used but the jasminaldehyde selectivity reduced due to poor stirring efficiency. Furthermore, the molar ratio of benzaldehyde and heptanal also had significant effect on the reaction performance (both conversion and selectivity).

In 2013, Prabhu and Palanichamy fabricated Al-KIT-6 mesoporous catalyst which was suitable to be used in the synthesis of jasminaldehyde (Prabhu and Palanichamy, 2013). They found that the activation of heptanal by the Brønsted acid sites was shown to be very crucial to allow the progress of this reaction. Among the Al-KIT-6 catalysts with various Al contents prepared, Al-KIT-6(150) had the best reaction conversion and jasminaldehyde (77.12% and 92%, respectively) at 120 °C for 12 h.

Sharma et al. synthesized amine and diamine functionalized magnesium organosilicate catalysts which contained strong basic site (Sharma et al., 2008). However, these catalysts can only be used in the synthesis of jasminaldehyde *via* condensation of heptanal with benzaldehyde under mild temperature condition because organoamine groups degraded at high temperature. They observed that the heptanal conversion was enhanced when the basicity of the catalysts increased; at 125 °C for 8 h, 99% conversion and 80% selectivity of jasminaldehyde were recorded.

Alireza et al. explored amine-functionalized SiO₂-Al₂O₃ mixed-oxide samples with various SiO₂/Al₂O₃ molar ratios (Alireza et al 2010). The samples were then used as catalysts in the solvent-free aldol condensation of heptanal using various types of aldehyde. The heptanal conversion increased with increasing the basicity of the solid catalysts. The results also showed that SiO₂/Al₂O₃ molar ratio of the catalysts played a significant role in the product selectivity and reactant conversion.

The catalytic performance of this aldol condensation using different types of acidic and basic solid catalysts under reflux condition was also reported and it is summarized in Table 2.2 (Wang et al., 2006; Alireza et al 2010). Essentially, heterogeneous acid catalysts show the lowest jasminaldehyde selectivity whereas

heterogeneous basic catalysts give higher heptanal conversion with better jasminaldehyde selectivity. In short, base catalyst is a more suitable candidate in this reaction than acid catalyst.

Table 2.2

Aldol condensation catalyzed using of various solid acid and base catalysts under reflux condition.

Catalyst	t (h)	T (°C)	Conv. (%)	Jasminaldehyde selectivity (%)
H-Beta	6	125	93	21 (Wong, et. al. 2018)
Al-MCM-41	10	125	75	29 (Surati et.al 2012)
Chitosan	8	125	94	82 (Sudheesh et. al. 2010)
MgO	8	125	98	76 (Sharma, et al .2010)
Hydrotalcite	8	125	98	86 (Sharma, et al 2010)

2.5 Heating methods

2.5.1 Reflux heating

Reflux encompasses heating the chemical reaction for a specific period (Aditha et al. 2016). For reflux heating, the reactants used must be in liquid form. The temperature used in the reaction is depending on the boiling point of solvents where a condenser is connected with water flow to allow condensation of solvent to occur (Figure 2.9) (Karakassides et al. 2000). Many chemical reactions take very long time for completing the reaction. Hence, high temperature is applied to accelerate the reactions. One should take note that usually the organic solvents are volatile and they can be flammable when heated to a high temperature, causing fire and explosion. Therefore, proper cooling on the condenser is very important to prevent excessive evaporation of solvent until the reaction vessel dries.